Image Cover Sheet

CLASSIFICATION	SYSTEM NUMBER 503806
UNCLASSIFIED	

TITLE

SHEAR SPEED GRADIENTS AND RESONANCES IN OCEAN SEISMO-ACOUSTIC MODELLING

System Number:

Patron Number:

Requester:

Notes:

DSIS Use only:

Deliver to:

Shear Speed Gradients and Resonances in Ocean Seismo-acoustic Modelling

David M.F. Chapman
Defence Research Establishment Atlantic
P.O. Box 1012, Dartmouth, Nova Scotia
B2Y 3Z7, Canada
Email: dave.chapman@drea.dnd.ca

ABSTRACT

Measurements of infrasonic seismo-acoustic ambient noise with an ocean bottom seismometer (OBS) in shallow water have uncovered an unusual phenomenon: the noise spectrum of the horizontal component of seabed velocity shows several prominent evenly-spaced peaks in the frequency range 0–8 Hz, whereas the noise spectra of both the acoustic pressure and the vertical component of seafloor velocity show very weak—or nonexistent—features at the same frequencies. Using an elastic multi-layer plane-wave propagation model implemented in *Mathematica*®, these features are attributed to shear-wave resonances in the upper sediment, which consists of layers of clay and silt of low shear speed (7–150 m/s) overlying a much faster glacial till layer. Not surprisingly, the frequency spacing Δf of successive resonances appears to be governed by the two-way travel time through the sediment; however, the frequency of the fundamental resonance is highly dependent upon the profile of shear speed versus depth. For example, a single isospeed layer generates resonances at $(n - 1/2)\Delta f$ but a power-law profile of the form $c_s(z) = c_0 z^{\nu}$ generates the observed $n\Delta f$ sequence more closely. The power-law profile for this site has been independently validated by fitting modelled group speed curves to measured interface wave dispersion data. In the computational model, the continuous coupling between p-waves and s-waves demanded by the correct physics of this problem is approximated by invoking many homogeneous sub-layers. It is remarkable that sediments with such a low shear speed display such a large seismic effect and that the effect is so sensitive to the nature of the shear speed profile.

1. Introduction

Shear waves in marine sediments have proved to be a significant factor in bottom-interacting ocean acoustics, in some environments. **[Hovem *et al.* 1991]** Specifically, **[Hughes *et al.* 1991]** have shown that shear wave resonances in a thin sediment layer over a rock substrate have a profound effect on acoustic reflection loss and shallow water acoustic transmission loss. In that study, it was adequate to model the thin sediment layer as a single homogeneous layer with average properties; however, others have argued that gradients in material properties cannot be ignored. **[Jensen 1991, Robins 1994, Hall 1995]** This paper presents experimental evidence of a seabed resonance phenomenon involving shear waves in surficial sediments for which the theoretical explanation depends critically on the shear speed gradient. The experiment consisted simply of measuring the

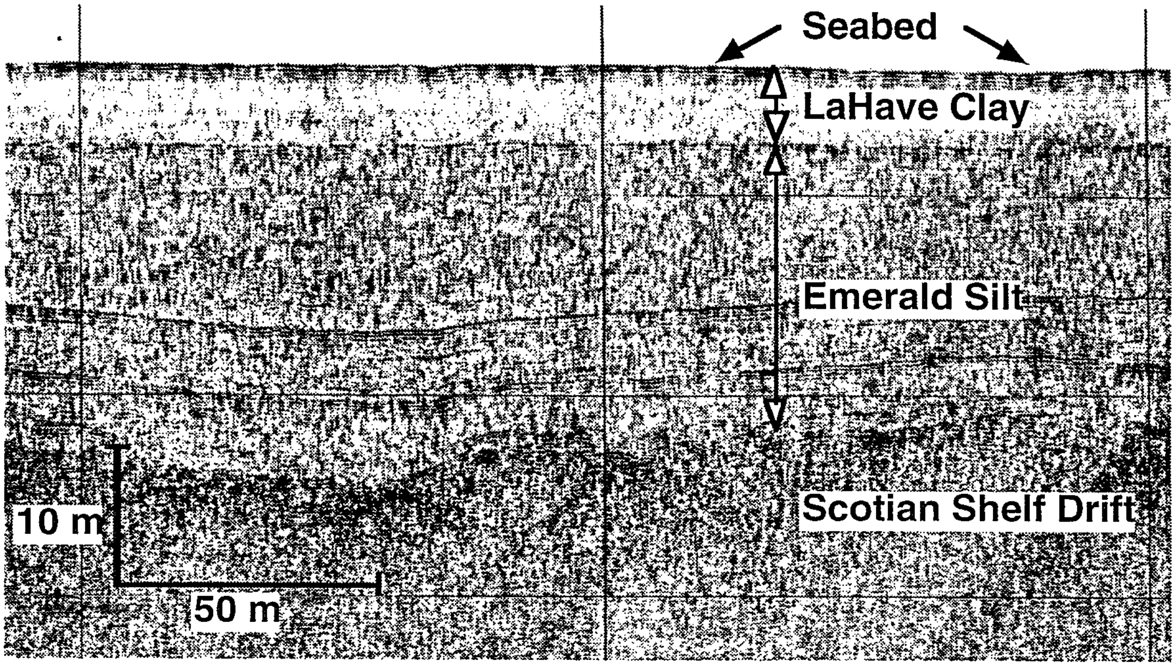

Figure 1: Seismic reflection profile of the surficial sediments at site ES.

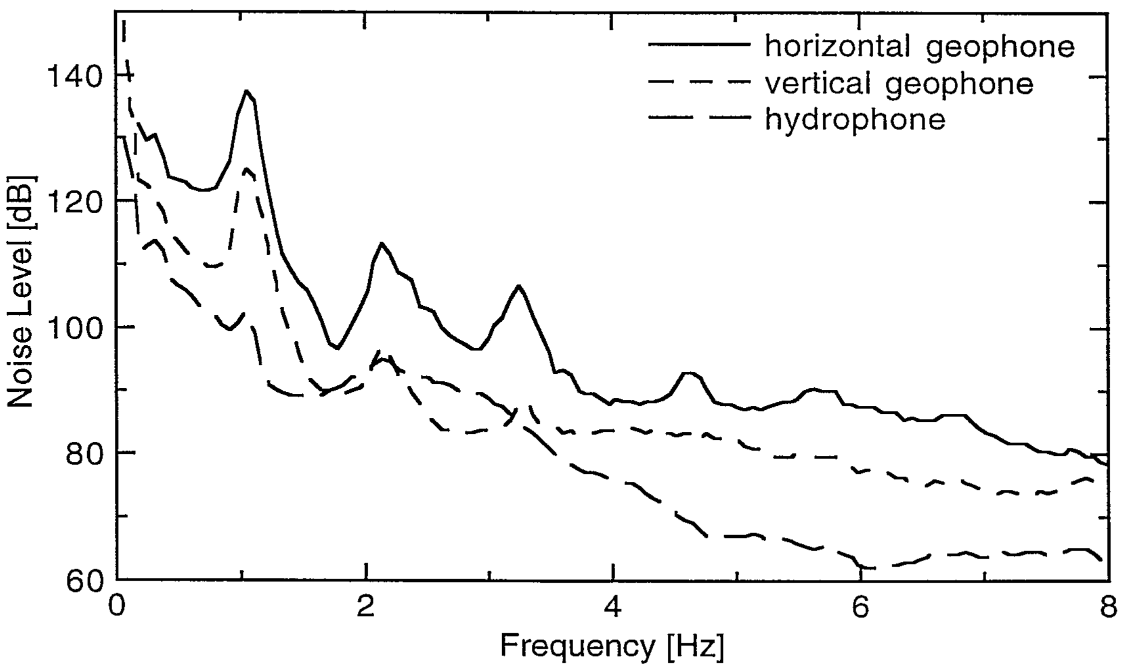

Figure 2: *Seismo-acoustic ambient noise resonances measured by an ocean bottom seismometer at site ES. The resonances are very strong on the horizontal geophone, noticeable on the vertical geophone, and almost nonexistent on the hydrophone. (Noise level units are dB re 1 $(nm/s)^2/Hz$ for the geophones and dB re 1 $\mu Pa^2/Hz$ for the hydrophone.)*

seismo-acoustic ambient noise field at the seabed using an ocean bottom seismometer (OBS). The OBS was equiped with geophones for measuring the particle velocity at the top of the sediment layer and a hydrophone for measuring the pressure in the water layer just above. Interestingly, we observed large resonance effects on the horizontal geophone, but these resonances were absent on the hydrophone. In this paper, we are not so concerned with the seismo-acoustic noise field itself, its source mechanisms, or modelling its spectrum; these topics are covered in a good review by [**Orcutt *et al.* 1993**]. We are more interested in how the noise field interacts with the seabed, and the insight this provides into the seismo-acoustics of the seafloor.

First we present the experimental data showing the seafloor noise resonances and a description of the environment. Then, we outline the theoretical method for computing the transfer function between an incident plane wave and the OBS sensors. As inputs for this computational model, we construct some geo-acoustic models of the environment and attempt to explain some features of the observed data. Finally, we draw some conclusions regarding the interplay of the various model parameters, the most significant being the profile of shear speed vs. depth in the sediment.

2. Experiment: Resonances in Seismo-acoustic Ambient Noise

In 1993, the Defence Research Establishment Atlantic (DREA) built and tested an OBS to investigate the geophone as a sensor for ocean acoustics experiments. [**Chapman *et al.* 1994, Dodds *et al.* 1994, Osler *et al.* 1994**] Many experimental sites were visited on several cruises, including a site not far from the Eastern Shore coastal region of Nova Scotia (site ES) and a site in the Emerald Basin (site EB), both on the Scotian Shelf. Seismo-acoustic propagation, ambient noise, and interface wave experiments were conducted at these sites. The interface wave dispersion data (i.e. group speed vs. frequency) was inverted to produce shear speed vs. depth profiles in the seabed. [**Osler and Chapman 1996**]

Both sites are in basins whose water depth is about twice as deep as the surrounding sand banks, and whose surficial sediment is composed of layers of clay and silt over a harder material, probably glacial till. [**Osler and Chapman 1996, King 1970**] At site ES, the water depth is 156 m and the clay/silt layer is about 25.5 m thick. At site EB, the water depth is 215 m and the clay/silt layer is about 38 m thick. (The EB clay/silt layer is possibly thicker than this, as the lower boundary is not distinct on the seismic profile record.) Figure 1 is a seismic reflection profile of site ES. The shear speed profile at this site was found to have the approximate form $c_s = 21.5z^{0.60}$(SI units), the shear speed varying from 21.5 m/s at 1 m depth to 150 m/s at the top of the till layer at 25.5 m depth.

Of particular interest at site ES are the resonance features in the seismo-acoustic ambient noise measured by the OBS on the seabed, shown in Figure 2. We observed these features with the DREA OBS on two visits, but we initially saw them with a borrowed OBS. The resonances in the noise on the horizontal geophone are quite noticeable: the first five peaks are at 1.03, 2.10, 3.21, 4.62, and 5.63 Hz, which are closely approximate a harmonic progression with a fundamental frequency of 1.09±0.05 Hz. Only one horizontal channel is shown; the others are similar. The vertical channel displays the same features, but they are much weaker, showing only the first three peaks. On the hydrophone channel, there is only a suggestion of a resonance at the fundamental frequency. Although the geoacoustic profile of site EB is quite similar, no resonant features have been observed in the ambient noise at that site. **[Dorman *et al.* 1993]** have published OBS noise spectra showing noticeable peaks on the horizontal geophone in the same frequency band (with a smoother and quieter noise spectrum on the vertical geophone), but they made no remarks about the features.

The cause of these noise resonances was not immediately evident. At first, we suspected them to be instrument-related, but their appearance at the same site at different times with different instruments convinced us that they are environmental features. We now believe that these peaks in the horizontal motion are caused by vertically-polarized shear waves resonating in the clay/silt layers. At this time, we do not have a complete model of the phenomenon, but the following sections will examine seismo-acoustic propagation in this environment and the role of the shear speed gradient in placing the modelled resonances at the appropriate frequencies.

3. Theory: Propagation in a Multi-layered Elastic Medium

Our hypothesis for the observed features of the seismo-acoustic noise field assumes a diffuse infrasonic noise field in the water column that is horizontally isotropic, but may have some vertical directionality. This noise field interacts with the elastic seabed and generates vertically-polarized shear waves at the boundaries between dissimilar layers. However, previous analysis of similar problems suggests that the strongest generation of shear waves would occur at the large impedance contrast at the sediment/substrate boundary. **[Chapman and Chapman 1993]** Subsequent multiple transits of the sediment layer by the shear waves give rise to resonances at frequencies that favour constructive interference. (Note that the lower boundary is necessary both to generate the shear waves and to provide a distinct layer thickness to form the resonances.) For the very low shear speeds in the clay sediments at site ES, we expect a negligible effect on the acoustic reflection coefficient, hence we would not expect the hydrophone to show large resonance effects. However, the geophones of an OBS are capable of sensing the seabed motion associated with shear waves, so resonances would be seen in the geophone ambient noise, although they would be more noticeable on the horizontal geophones than on the vertical geophones, as we explain below.

At first thought, it may seem paradoxical that vertically-polarized shear waves would give rise to large horizontal motion and small vertical motion at the seafloor, but the paradox is resolved by realizing that the shear-wave particle motion at the water/sediment boundary is the sum of an upward-travelling incident and a down-ward-travelling reflected shear wave. For low shear speeds, the shear wave is almost perfectly reflected with a phase inversion.

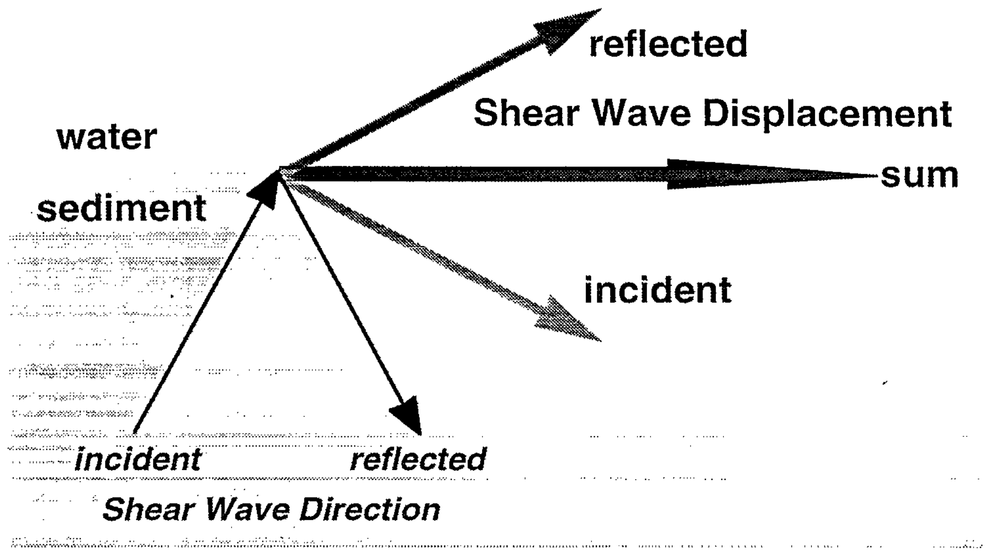

Figure 3: *A vertically-polarized shear wave in a low-shear sediment undergoes nearly perfect reflection at the sediment/water boundary with a phase inversion, causing the net displacement at the boundary to be very large in the horizontal direction.*

As illustrated in Figure 3, this gives rise to a net displacement that is very large in the horizontal direction and substantially reduced in the vertical direction.

If the shear speed profile in the sediment layers were truly continuous, the problem would become very difficult, as gradients of shear modulus give rise to continual coupling between shear (s) and compressional (p) waves. **[Robins 1994]** Indeed, the fundamental equations of motion in such a medium do not naturally decouple into a wave equation for a p wave and another wave equation for an s wave. The conventional solution to this difficulty is to imagine the continuous profile to be approximated by a sequence of fine homogeneous sub-layers. If the number of sub-layers is sufficiently large, the net effect of the many discrete boundary interactions should approximate the physics of the continuous profile. (However, just how many layers are needed is not well understood; we propose that no sub-layer should be larger than a fraction of a shear wavelength, that fraction being between one-eighth and one-quarter.)

To investigate the physics of the observed ambient noise resonances, we will calculate the transfer function between the longitudinal motion (particle velocity) of a plane p wave in the water incident on the seabed and three motions at the water/seabed boundary: (1) the acoustic pressure in the water (divided by the acoustic impedance to give an equivalent velocity), (2) the vertical velocity of the boundary, and (3) the horizontal velocity of the sediment layer at the boundary. These transfer functions relate to the observed signals on the hydrophone, the vertical geophone, and the horizontal geophone, respectively. The vertical and horizontal motions of the boundary are combinations of p and s waves travelling both up and down in the topmost sediment layer. As the seabed is composed of multiple elastic layers of varying properties, all the effects of reflections from deeper boundaries must be included in the calculation of the fields at the ocean floor.

We follow **[Brekhovskikh 1980]** in his calculation of the reflection coefficient of a multi-layered elastic medium, with some adaptations. We imagine a plane wave of frequency ω and horizontal wavenumber k incident upon a stack of elastic layers. (All the fields in all the layers will share the same horizontal wavenumber, due to Snell's law.) The particle velocity $\mathbf{u}$ in a given layer with compressional speed c_{p} and shear speed c_{s} is given by the vector expression

$$\begin{aligned}\mathbf{u} &= (c_{\mathrm{p}} / \omega)\left[a_{\mathrm{p}}(k\hat{\mathbf{x}} + q_{\mathrm{p}}\hat{\mathbf{z}})e^{i(kx+q_{\mathrm{p}}z)} + b_{\mathrm{p}}(k\hat{\mathbf{x}} - q_{\mathrm{p}}\hat{\mathbf{z}})e^{i(kx-q_{\mathrm{p}}z)}\right] \\ &+ (c_{\mathrm{s}} / \omega)\left[a_{\mathrm{s}}(q_{\mathrm{s}}\hat{\mathbf{x}} - k\hat{\mathbf{z}})e^{i(kx+q_{\mathrm{s}}z)} + b_{\mathrm{s}}(q_{\mathrm{s}}\hat{\mathbf{x}} + k\hat{\mathbf{z}})e^{i(kx-q_{\mathrm{s}}z)}\right],\end{aligned} \tag{1}$$

in which a_{p}, b_{p}, a_{s}, and b_{s} are the amplitudes of downward-travelling (a) and upward-travelling (b) p and s waves at the top of the layer; $\hat{\mathbf{x}}$ and $\hat{\mathbf{z}}$ are the unit vectors in the horizontal and downward vertical directions; and q_{p} and q_{s} are the compressional and shear vertical wavenumbers given by

$$q_{\mathrm{p}} = \sqrt{(\omega/c_{\mathrm{p}})^2 - k^2} \quad \text{and} \quad q_{\mathrm{s}} = \sqrt{(\omega/c_{\mathrm{s}})^2 - k^2}. \tag{2}$$

The compressional and shear components of $\mathbf{u}$ satisfy the compressional and shear wave equations and represent longitudinal motion and vertically-polarized transverse motion, respectively. From this field, the relevant velocity and stress components at the top of a layer are:

$$u_x = (c_{\mathrm{p}} / v)(a_{\mathrm{p}} + b_{\mathrm{p}}) + \sqrt{1-(c_{\mathrm{s}} / v)^2}(a_{\mathrm{s}} + b_{\mathrm{s}}), \tag{3a}$$

$$u_z = \sqrt{1-(c_{\mathrm{p}} / v)^2}(a_{\mathrm{p}} - b_{\mathrm{p}}) - (c_{\mathrm{s}} / v)(a_{\mathrm{s}} - b_{\mathrm{s}}), \tag{3b}$$

$$\tau_{zz} = i\omega v\rho\left[2(c_{\mathrm{p}} / v)(1-2c_{\mathrm{s}}^2 / v^2)(a_{\mathrm{p}} + b_{\mathrm{p}}) - 2(c_{\mathrm{s}}^2 / v^2)\sqrt{1-(c_{\mathrm{s}} / v)^2}(a_{\mathrm{s}} + b_{\mathrm{s}})\right], \tag{3c}$$

$$\tau_{xz} = i\omega v\rho\left[2(c_{\mathrm{s}}^2 / v^2)\sqrt{1-(c_{\mathrm{p}} / v)^2}(a_{\mathrm{p}} - b_{\mathrm{p}}) + (c_{\mathrm{s}} / v)(1-2c_{\mathrm{s}}^2 / v^2)(a_{\mathrm{s}} - b_{\mathrm{s}})\right], \tag{3d}$$

in which $v = \omega / k$ is the horizontal phase speed and ρ is the bulk density of the layer. The associated velocity and stress components at the bottom of the layer of thickness h are obtained from Eqs. (3a–3d) by the substitutions

$$a_{\mathrm{p}} \to a_{\mathrm{p}}e^{i\varphi_{\mathrm{p}}}, \quad a_{\mathrm{s}} \to a_{\mathrm{s}}e^{i\varphi_{\mathrm{s}}}, \quad b_{\mathrm{p}} \to b_{\mathrm{p}}e^{-i\varphi_{\mathrm{p}}}, \quad \text{and } b_{\mathrm{s}} \to b_{\mathrm{s}}e^{-i\varphi_{\mathrm{s}}}, \tag{4}$$

in which

$$\varphi_p = (\omega h / c_p)\sqrt{1-(c_p / v)^2} \text{ and } \varphi_s = (\omega h / c_s)\sqrt{1-(c_s / v)^2} \quad (5)$$

Across the boundary between two adjacent elastic layers (assumed to be "welded"), the four velocity and stress components must be continuous. For a system of n layers consisting of $n-2$ finite layers sandwiched between two semi-infinite layers, there are $4n$ field variables, for which the $n-1$ boundaries provide $4n-4$ equations; however, there are four additional constraints, as the incident amplitudes in the semi-infinite layers must be specified. This leaves a system of $4n-4$ equations with $4n-4$ unknowns. In practice, we usually consider simple incident fields, such as an incident p wave in the uppermost layer; i.e. the constraints would be $a_p^{(1)} = 1$, $a_s^{(1)} = 0$, $b_p^{(n)} = 0$, and $b_s^{(n)} = 0$, in which the superscript denotes the layer number. If a layer is fluid, the number of amplitudes and boundary conditions is reduced, as shear waves are not supported $(a_s = b_s = 0)$ and a "slip" condition exists at the layer boundaries, so that u_x need not be continuous across them. For the application in this paper, the first layer is a fluid (the ocean); also, we are only interested in the reflected pressure in the ocean layer and the vertical and horizontal motions at the top of the second (surficial sediment) layer. Consequently, many amplitudes may be eliminated from the equations, leaving only five amplitudes to be determined, i.e $b_p^{(1)}$, $a_p^{(2)}$, $b_p^{(2)}$, $a_s^{(2)}$, and $b_s^{(2)}$.

In vector form, the solution of this problem amounts to the inversion of a large block-diagonal matrix with many zero off-diagonal elements. (The boundary conditions only connect adjacent layers.) There are several methods of solution available, but we chose to code the problem in *Mathematica*® and allow the LinearSolve procedure choose the optimal method. **[Wolfram 1996]** The user chooses the type of incident wave (p or s), the incident layer (upper or lower half-space), the desired output sensor (hydrophone, vertical geophone, or horizontal geophone), and the layer thicknesses, densities, and wave speeds (both compressional and shear). Bulk attenuation of the waves within the layers is handled by adding appropriate small imaginary parts to the wave speeds. The computer model constructs the matrix of boundary condition equations stage, but the elements are still functions of frequency and horizontal phase speed (or grazing angle). The desired output is then computed as a function of frequency and/or grazing angle and a plot of the transfer function is generated. In this paper, we choose a typical grazing angle and plot the magnitude of the transfer functions (in dB) vs. frequency. We partly validated the *Mathematica*® computer code by comparing calculated reflection and transmission coefficients at a fluid/solid boundary with published results. **[Ergin 1952]**

4. Model: Effect of Shear Wave Gradient on Resonance

To explain the observed resonances in the seismo-acoustic noise field, we must construct a plausible model of the geo-acoustic environment and calculate the transfer function between plane-wave components of the incident noise field and the OBS sensors. It is probable—although not certain—that the source of the noise at these frequencies is in the ocean; however we must allow for the possibility that the noise may come from beneath the seabed either as p waves or s waves. As the shear speeds in the upper layers are small compared with the sound speed in water, the propagation angles of the shear waves should be quite steep (i.e. large grazing angles) and should not vary significantly as the incidence angle changes. This is desirable, for otherwise the resonance structure would be sensitive to the grazing angle of the incident waves and would likely become smeared out if the incident field were diffuse.

4.1 Single homogeneous layer

Previous modelling efforts involving shear wave resonances in seabed reflection loss calculations enjoyed considerable success with the simple assumption of a single homogeneous layer with average properties. **[Chapman and Chapman 1993]** We estimate the two-way travel time through the layer of thickness H to be the inverse of the resonance spacing, so the average shear speed is then $\bar{c}_s = 2H\Delta f$, which turns out to be $2 \times 25.5 \times 1.09 = 55.6$ m / s in this case. Table I gives the geo-acoustic parameters for a simple 3-layer model (water/"clay"/till) based on this premise and Fig. 4 shows the modelled transfer functions at the OBS for a p-wave incident from the water side at 30 degrees grazing angle, calculated as described above. The resonances we are looking for are prominent on the horizontal geophone, substantially reduced on the other sensors, and they have nearly the right frequency separation, but the fundamental is at the wrong frequency. The modelled sequence is closer to $(n - 1/2)\Delta f$, consistent with a constructive interference condition that includes a phase shift of π for every two-way transit of the layer. (This we have: the shear wave inverts at the clay/water boundary.) In other words, the model is doing more or less what it we expect it should; it simply doesn't agree with the observations! Despite its shortcomings, however, this too-simple geoacoustic model at least simulates a strong response of the horizontal geophone

4.2 Multiple layers approximating a power-law shear speed profile

The shortcoming of the single homogeneous sediment layer suggests some sort of multi-layer model, possibly an approximation to a continuous profile. Sensitivity studies with the computer code show that results are very sensitive to the shear speed values and (to a lesser extent) the shear attenuation values, but are quite insensitive to the other parameters. This is also true for the interface wave dispersion analysis carried out at the same site. **[Osler and Chapman 1996]** Accordingly, an obvious candidate for a multi-layer clay/silt model would be the 9-layer staircase approximating the continuous power-law shear speed profile

Table I: Geo-acoustic parameters of a 3-layer water/clay/till model

layer	thickness [m]	p-wave speed [m/s]	s-wave speed [m/s]	p-wave attenuation [dB/λ]	s-wave attenuation [dB/λ]	density (relative to water)
water	∞	1490	–	0	–	1.00
clay	25.5	1500	55.6	.35	1.25	1.56
till	∞	2000	900	.50	1.00	2.10

Table II: Geo-acoustic parameters of an 11-layer water/clay/silt/till model

layer	thickness [m]	p-wave speed [m/s]	s-wave speed [m/s]	p-wave attenuation [dB/λ]	s-wave attenuation [dB/λ]	density (relative to water)
water	∞	1490	–	0	–	1.0
clay 1	.25	1450	**7.5**	0.2	1.0	1.5
clay 2	.25	1450	**12**	0.2	1.0	1.5
clay 3	1.0	1450	**21**	0.2	1.0	1.5
clay 4	1.5	1450	**36**	0.2	1.0	1.5
clay 5	2.5	1450	**51**	0.2	1.0	1.5
silt 1	3.5	1550	**71**	0.5	1.5	1.6
silt 2	4.5	1550	**95**	0.5	1.5	1.6
silt 3	6.0	1550	**124**	0.5	1.5	1.6
silt 4	6.0	1550	**130**	0.5	1.5	1.6
till	∞	2000	900	0.5	1.0	2.1

generated by that analysis. The full geo-acoustic model for this environment is shown in Table II, and the corresponding transfer functions are shown in Figure 5. For this geo-acoustic model, the resonances are much closer to the sequence $n\Delta f$. The frequencies of the experimental noise peaks are compared to the frequencies of the transfer function peaks in Table III. The shear wave profile used for this calculation was previously derived from the interface wave dispersion data, and no attempt has been made to "fit" the resonances better by "adjusting" the shear speed values in the layers. (There is no obvious reason why the experimental peaks should be an exact harmonic sequence; it must be a coincidence.)

4.3 Sensitivity studies: alterations to the successful geo-acoustic model

With the computational model described, we performed many variations on the above calculation, but space limitations do not permit an exhaustive presentation of the evidence for the findings summarized in point form below:

• The frequencies and levels of the transfer function peaks are insensitive to variations (within reasonable bounds) of the layer densities and compressional speeds. Consequently, gradients in these quantities (leading to small layer-to-layer differences) have an insignificant—although detectable—influence.

• The frequencies of the transfer function peaks are insensitive to the grazing angle of the incident wave. As a complete model of this phenomenon would incoherently integrate energy from all plane-wave components of a diffuse incident field, this invariance of the peak frequencies ensures that the resonance structure would be maintained when generalizing the single-plane-wave case into the diffuse case.

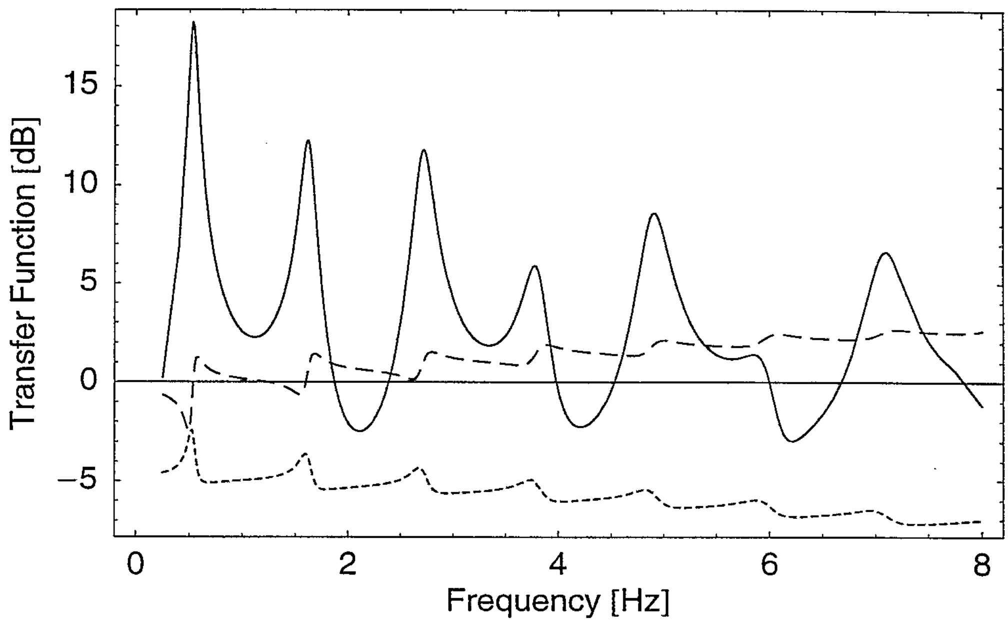

***Figure 4:** OBS transfer functions modelled using a single sediment layer: horizontal geophone (solid line), vertical geophone (short dash), and hydrophone (long dash)*

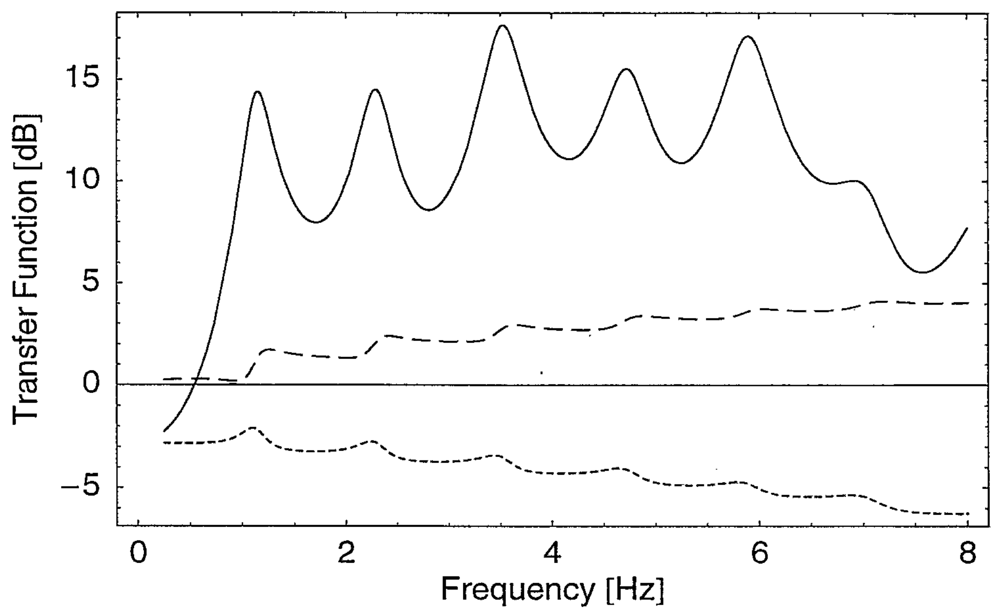

***Figure 5:** OBS transfer functions modelled using multiple sediment layers: horizontal geophone (solid line), vertical geophone (short dash), and hydrophone (long dash)*

Table III: Measured and modelled resonance frequencies

model or experiment	f1 [Hz]	f2 [Hz]	f3 [Hz]	f4 [Hz]	f5 [Hz]
experiment	1.03	2.10	3.21	4.62	5.63
11-layer model	1.13	2.29	3.53	4.69	5.74

• The transfer function resonances are just as prominent for p waves and s waves incident from beneath the layered system. A complete model of the infrasonic seismo-acoustic noise field (at least for the horizontal geophone sensor) would have to consider the possibility that noise could arrive from other than ocean-borne sources.

• A linear (rather than a power-law) shear-speed gradient gives a similar transfer function resonance sequence, although we could not improve on the match provided by the power-law profile.

• If the 9-layer clay/silt shear speed staircase is viewed as an approximation to a continuous profile, then the subdivision of sediment layers has not converged: synthesis of 9-layer, 18-layer, and 36-layer staircases based on the same power-law profile show different results, especially at the upper frequencies. We made each sub-layer thickness proportional to the shear wavelength in that sub-layer. For a monotonically-increasing shear speed profile, this yields a sequence of layers of increasing thickness. Although we have not proven this to be the optimal arrangement, it seems to significantly reduce the total number of layers required to achieve convergence. Part of the problem with slow convergence with the power-law profile is the very small shear speeds near z=0, which generate very thin sub-layers.

5. Summary and Conclusions

We have observed unusual peaks in the horizontal component of infrasonic seismo-acoustic noise measured with an ocean bottom seismometer mounted on a seabed composed of multiple layers of clay and silt over a hard glacial till substrate. Modelling the geo-acoustic environment as a stack of elastic layers, we have calculated the transfer functions between an arbitrary plane wave incident on the layered system and the sensor outputs of an OBS at the seafloor. Modelling results support the hypothesis that the observed peaks are caused by vertically-polarized low-speed shear waves resonating in the sediment layers between the ocean and the till. The model confirms that the effect on the vertical motion and a water-borne pressure sensor would be significantly lower. Although the frequency separation of the peaks can be reproduced using a single homogeneous sediment layer with average properties, the offset of the modelled peaks is incorrect: the single sediment layer shows an approximate $(n-1/2)\Delta f$ sequence while the data shows an approximate $n\Delta f$ sequence. The correct sequence is realized by an independently-derived multi-layered shear speed profile which suggests a continuous power-law profile of the form $c_s(z) = c_0 z^{\nu}$. The gradient in the shear speed profile seems to play a key role in the physics of this problem. Furthermore, the large number of sub-layers required to achieve a convergent result for a hypothetical continuous shear speed profile suggests that continual coupling of shear and compressional waves may be a significant issue in ocean seismo-acoustics modelling (that is, if shear waves are needed at all). A complete model of this phenomenon would have to consider sources other than those within the ocean, as the transfer function model predicts that p waves or s waves from below the layered system can give rise to similar features in the spectrum.

Acknowledgments

The author is grateful to Dave Heffler of the Atlantic Geoscience Centre/Bedford Institute of Oceanography for the loan of the OBS used on the sea test that discovered the seismo-acoustic noise resonances. The contribution of John Osler (currently at the SACLANT Undersea Research Centre, Italy) to the DREA OBS project was invaluable, and the author thanks him for the constant encouragement to write up this portion of the work.

References

Brekhovskikh, L.M., *Waves in Layered Media, Second Edition*, translated by Robert T. Beyer (Academic Press, New York, 1980).

Chapman, D.M.F., J.C. Osler, W.C. Risley, and J.C. Dodds, "Underwater acoustic measurements with a digital ocean bottom seismometer" (A), J. Acoust. Soc. Am. **96**, 3330 (1994).

Chapman, N. Ross, and David M.F. Chapman, "A coherent ray model of plane-wave reflection from a thin sediment layer," J. Acoust. Soc. Am. **94**, 2731–2738 (1993).

Dodds, D.J., D.M.F. Chapman, J.C. Osler, and W. Cary Risley, "Minimizing instrument effects in an ocean bottom seismometer," Canadian Acoustics **22**, 161-162 (1994).

Ergin, Kazim, "Energy ratio of the seismic waves reflected and refracted at rock-water boundary", Bull. Seism. Soc. Am. **42**, 349-371 (1952).

Hall, Marshall V., "Acoustic reflectivity of a sandy seabed: A semianalytic model of the effect of coupling due to the shear modulus profile", J. Acoust. Soc. Am. **98**, 1075-1089 (1995).

Hovem, Jens M., Michael D. Richardson, and Robert D. Stoll, (eds.), *Shear Waves in Marine Sediments*, (Kluwer, Dordrecht, 1991).

Hughes, Steven J., Dale D. Ellis, David M. F. Chapman, and Philip R. Staal, "Low-frequency acoustic propagation loss in shallow water over hard-rock seabeds covered by a thin layer of elastic-solid sediment," J. Acoust. Soc. Am. **88**, 283-297 (1990).

Jensen, Finn B., "Excess attenuation in low-frequency shallow-water acoustics: a shear wave effect?", in **[Hovem *et al.* 1991]**, 421-430.

King, L.H., *Surficial Geology of the Halifax-Sable Island map area, Marine Science Paper 1*, (Department of Energy, Mines and Resources, Ottawa, 1970).

Orcutt, John A., Charles S. Cox, Alick C. Kibblewhite, W.A Kuperman, and Henrik Schmidt, "Observations and causes of ocean and seafloor noise at ultra-low and and very-low frequencies", in B. R. Kerman (ed.), Natural Physical Sources of Underwater Sound (Kluwer, Dordrecht), 203-232 (1993).

Osler, J.C., Chapman, D.M.F., Risley, W.C., Dodds, J.C., "In situ calibration of the coupling of an ocean bottom seismometer to sand and clay surficial sediments" (A), EOS transactions A.G.U. **75**, 419 (1994).

Osler, John C., and David M.F. Chapman, "Seismo-acoustic determination of the shear-wave speed of surficial clay and silt sediments on the Scotian Shelf", Canadian Acoustics **24**, 11–22 (1996).

Robins, A.J., "Generation of shear and compressional waves in an inhomogeneous elastic medium", J. Acoust. Soc. Am. **96**, 1669–1676 (1994).

Wolfram, Steven, *The Mathematica® Book, Third Edition* (Wolfram Media, Inc., Champaign, 1996).

#S03806